Spin waves at low temperatures in two-sublattice Heisenberg ferromagnets and ferrimagnets with different sublattice anisotropies

1997 J. Phys.: Condens. Matter 9 8101

(http://iopscience.iop.org/0953-8984/9/38/015)

J. Phys.: Condens. Matter **9** (1997) 8101–8118. Printed in the UK PII: S0953-8984(97)78444-3

Spin waves at low temperatures in two-sublattice Heisenberg ferromagnets and ferrimagnets with different sublattice anisotropies

Zhang Zhi-dong† and Zhao Tong

Institute of Metal Research, Academia Sinica, Wenhua Road 72, Shenyang 110015, People's Republic of China, and

International Centre for Material Physics, Academia Sinica, Wenhua Road 72, Shenyang 110015, People's Republic of China

Received 7 October 1996, in final form 14 July 1997

Abstract. The Hamiltonian for two-sublattice Heisenberg ferromagnets and ferrimagnets with different sublattice anisotropies, which is applicable for rare-earth–transition-metal (R–T) intermetallics, is established. In order to study spin-waves in easy plane or easy cone configuration, a transformation of spin-vector coordinates is performed by rotating the quantization axis frame by Eulerian angles and accordingly the Hamiltonian. Spin-wave spectra at low temperatures of the present system are determined by performing the standard Holstein–Primakoff transformation and a four-step diagonalizing procedure consisting of two coupled Cullen transformations, an extended Bogoliubov transformation, two independent Bogoliubov transformations and two independent Holstein–Primakoff transformations. The results for the ground states of the easy axis, the easy plane and the easy cone configurations are compared with those obtained by the mean-field theory. The border lines between the different spin structures are derived in either the pure classical limit or the large-exchange limit. Continuous transitions, accompanied with the continuous change of the angle between the averaged sublattice magnetizations, are found in both cases. It is found that splittings of the spin-wave spectra of the two-sublattice Heisenberg ferromagnets or ferrimagnets exist. A gap can appear in the spin-wave spectra, depending on the competition among the exchange and the anisotropies. Other physical properties, such as sublattice magnetization and specific heat, are discussed also.

1. Introduction

Rare-earth (R)–transition metal (T) intermetallics have attracted great interest due to their outstanding permanent magnetic properties [1], which, in most cases, can be satisfactorily explained by a phenomenological two-sublattice model [2–4]. This model simply treats the total contribution of the magnetic properties as arising separately from the rare-earth and the transition-metal sublattices, considering R–T exchange interaction between the moments of the two sublattices. For light rare-earth elements, the R–T exchange results in the ferromagnetic coupling of the moments of the two sublattices. For heavy rare-earths, it favours an antiparallel (i.e., ferrimagnetic) alignment of the moments. In recent years, many experiments have shown the existence of anisotropies in both sublattices, which play an important role in determining the magnetic properties of such materials. These give an impetus to theoretical investigation on this subject.

† Correspondence to Zhang Zhi-dong, Institute of Metal Research, Academia Sinica, Wenhua Road 72, Shenyang 110015, People's Republic of China. Fax: +86 24 3891320.

0953-8984/97/388101+18$19.50

It is usually assumed that the R–T exchange is strong enough to couple collinearly the moments of the sublattices at zero magnetic field. A recent work showed that in a two-sublattice system there exist two different spin configurations in the absence of external field [5]. Depending on the competition among the exchange and the opposite anisotropies of the two sublattices, the canting spin structures may occur in either ferromagnetic or ferrimagnetic materials. The phase diagrams of the different spin configurations (i.e., the collinear and the non-collinear ones) at either zero or non-zero field have been determined by a mean-field analysis for the two-sublattice system [5, 6].

Besides the phenomenological approach, quantum models may be used to describe the magnetic properties of such a system. The most powerful approach is the mean-field–crystal-field (MF–CEF) approximation [7–10]. This description lies between an atomistic one, which describes the CEF upon the R ion by a Hamiltonian H_{CEF}, and a very simplified mean-field one to deal with the exchange interaction. This model treats the weaker anisotropy of the T sublattice within the phenomenological model. The limitation of this approach is that it is a computational one, fitting the experimental data by an adequate choice of the parameters involved. It hardly reveals the detailed physical processes involved in the complexity of the spin reorientation phenomenon.

The uniaxial (or non-uniaxial) Heisenberg model with nearest-neighbour, next-nearest-neighbour and even third-neighbour interactions has been the subject of great interest for more than ten years [11–14]. The main feature of the results obtained from these models is the large number of modulated structural phases arising from the variation of the interaction strengths and temperature. The spin wave spectrum at low temperatures is a main subject of the study of the Heisenberg antiferromagnets. The effects of single-ion uniaxial (or non-uniaxial) anisotropy on the magnetic properties of antiferromagnets have been extensively studied [15–17]. Investigations on two-sublattice ferromagnets or ferrimagnets with different sublattice single-ion anisotropies were made by various authors in the 1960s and early 1970s [18–31] for the rare-earths. Based on a one-sublattice model, del Moral used the spin-wave approximation to study the spin-reorientation transitions in the ferromagnetic systems with competing axial–planar anisotropies, i.e., the R–T intermetallics $(RE'_xRE_{1-x})_2Fe_{14}B$ and $(RE'_xRE_{1-x})Co_5$ [32, 33]. The transformation of spin vector coordinates, rotating the quantization axis frame by Eulerian angles (θ and ψ), was proposed by del Moral [32, 33] to deal with the spin waves for the easy plane or easy cone configuration.

The aim of this paper is to study the spin-wave spectra at low temperatures of two-sublattice Heisenberg ferromagnets and ferrimagnets with different sublattice anisotropies, which is applicable for the R–T intermetallics. The two sublattices (i.e., the R and the T ones) have different anisotropies, but also different spin amplitudes. Since the linear-spin-wave theory [34, 35] (the leading term in the $1/S$ expansion) gives fairly good results for the quantum corrections to various physical quantities [36–40], we shall treat the spin fluctuations within the linear-spin-wave theory. The Hamiltonian for two-sublattice Heisenberg ferromagnets and ferrimagnets with different sublattice anisotropies will be established in section 2. In order to study the spin waves in the easy plane or easy cone configuration, as proposed by del Moral [32, 33], the transformation of spin-vector coordinates, rotating the quantization axis frame by Eulerian angles (θ and ψ) and accordingly the Hamiltonian, and the standard Holstein–Primakoff transformation [41] will be performed. In section 3, spin-wave spectra at low temperatures of the present system will be determined by performing a diagonalizing procedure which consists of two coupled Cullen transformations [42], an extended Bogoliubov transformation [43], two independent Bogoliubov transformations [43] and two independent Holstein–Primakoff transformations [41]. The ground state and the spin-wave excitation for the easy axis, the easy plane and the easy cone configurations will be studied briefly in sections 4 and 5. Other physical properties, such as sublattice magnetization and specific heat, will be discussed in section 6. Section 7 is for concluding remarks.

2. Hamiltonian and rotate transformation

In this work, we investigate the two-sublattice Heisenberg ferromagnets and ferrimagnets with different sublattice anisotropies, modelled by the following Hamiltonian:

$$\boldsymbol{H} = -J\sum_{\langle i,j\rangle} \boldsymbol{S}_i \cdot \boldsymbol{S}_j - K_A \sum_i (S_i^z)^2 - K_B \sum_j (\boldsymbol{S}_j^z)^2 \tag{2.1}$$

where J is the isotropic exchange constant. A positive J is for ferromagnetic coupling whereas a negative J is for a ferrimagnetic one. K_A and K_B are the anisotropy constants for the sublattices A and B, respectively. A positive K_A (or K_B) favours an easy axis alignment of spins in the sublattice A (or B), whereas a negative value tends to the easy plane. To simplify, in this work, we neglect the anisotropies within the basal plane. $S_i = \langle S_i^x, S_i^y, S_i^z\rangle$ are operators belonging to the spin-S representation [46].

We restrict ourselves to the low-temperature region of $T \ll T_C$. The spin-wave approximation naturally assumes small spin deviations from the quantization axis. For the present system, the natural quantization axis is the averaged magnetization direction. If the system were near the easy axis configuration, it would be reasonable to assume that the original ferromagnetic state or Néel state is easy axis, in which all spins couple parallel or antiparallel to the z axis, but in the present system, other spin configurations, such as easy plane and easy cone ones, exist when the nonuniaxial anisotropy is dominant. For studying the spin waves in the easy plane or easy cone configuration, as proposed by del Moral [32, 33], one needs to rotate the quantization axis frame by Eulerian angles θ and ψ [32, 33, 44, 45].

By use of the Holstein–Primakoff transform [41] and the linear-spin-wave approximation [34, 35], retaining terms up to the second order in the boson operators a_i^+, a_i, b_j^+ and b_j, we have

$$\begin{aligned}\boldsymbol{H} = \boldsymbol{H}_0^0 &+ A\sum_i \boldsymbol{a}_i^+\boldsymbol{a}_i + B\sum_j \boldsymbol{b}_j^+\boldsymbol{b}_j + \frac{C}{Z}\sum_{i\delta}(\boldsymbol{a}_i\boldsymbol{b}_{i+\delta} + \boldsymbol{a}_i^+\boldsymbol{b}_{i+\delta}^+)\\ &+\frac{D}{Z}\sum_{i\delta}(\boldsymbol{a}_i\boldsymbol{b}_{i+\delta}^+ + \boldsymbol{a}_i^+\boldsymbol{b}_{i+\delta}) + A'\sum_i(\boldsymbol{a}_i^+\boldsymbol{a}_i^+ + \boldsymbol{a}_i\boldsymbol{a}_i) + B'\sum_j(\boldsymbol{b}_j^+\boldsymbol{b}_j^+ + \boldsymbol{b}_j\boldsymbol{b}_j)\\ &+\frac{A''}{\sqrt{N}}\sum_i(\boldsymbol{a}_i^+ + \boldsymbol{a}_i) + \frac{B''}{\sqrt{N}}\sum_J(\boldsymbol{b}_j^+ + \boldsymbol{b}_j).\end{aligned} \tag{2.2}$$

The parameters in (2.2) are shown in appendix A.

The Hamiltonian (2.2) is rewritten by introducing the Fourier transforms of the boson operators in the reduced Brillouin zone:

$$\begin{aligned}\boldsymbol{H} = \boldsymbol{H}_0^0 &+ A\sum_k \boldsymbol{a}_k^+\boldsymbol{a}_k + B\sum_k \boldsymbol{b}_k^+\boldsymbol{b}_k + C\sum_k \gamma_k(\boldsymbol{a}_k^+\boldsymbol{b}_k^+ + \boldsymbol{a}_k\boldsymbol{b}_k)\\ &+D\sum_k \gamma_k(\boldsymbol{a}_k^+\boldsymbol{b}_k + \boldsymbol{a}_k\boldsymbol{b}_k^+) + A'\sum_k(\boldsymbol{a}_k^+\boldsymbol{a}_{-k}^+ + \boldsymbol{a}_k\boldsymbol{a}_{-k})\\ &+B'\sum_k(\boldsymbol{b}_k^+\boldsymbol{b}_{-k}^+ + \boldsymbol{b}_k\boldsymbol{b}_{-k}) + A''(\boldsymbol{a}_0^+ + \boldsymbol{a}_0) + B''(\boldsymbol{b}_0^+ + \boldsymbol{b}_0).\end{aligned} \tag{2.3}$$

with

$$\gamma_k = \frac{1}{Z}\sum_{\delta} \mathrm{e}^{\mathrm{i}\boldsymbol{k}\cdot\boldsymbol{\delta}}. \tag{2.4}$$

3. Diagonalizing procedure

The Hamiltonian (2.3) is very complicated: different kinds of non-diagonal term exist. The bi-linear terms in the Hamiltonian (2.3) are similar to those of the second case denoted in [24], while the linear terms are similar to those in [32] and [33]. This Hamiltonian can be diagonalized by the following four-step diagonalizing procedure. First, two coupled Cullen diagonalization transformations [42] are employed to eliminate the linear terms in $\boldsymbol{a}_0^+$, $\boldsymbol{a}_0$; $\boldsymbol{b}_0^+$, $\boldsymbol{b}_0$ in equation (2.3). Second, an extended Bogoliubov transformation [43] is developed, which is asymmetrical for the positive and negative $\boldsymbol{k}$ spaces, so that the non-diagonal terms $\boldsymbol{a}_k^+\boldsymbol{b}_k^+$, $\boldsymbol{a}_k\boldsymbol{b}_k$, $\boldsymbol{a}_k^+\boldsymbol{b}_k$ and $\boldsymbol{a}_k\boldsymbol{b}_k^+$ can be eliminated. Third, two independent Bogoliubov transformations [43] are used and, finally, two independent Holstein–Primakoff transformations [41] are applied to remove the remains of the non-diagonal terms. The later three-step diagonalizing procedure is equivalent to the four-step diagonalizing procedure developed in [24].

3.1. The first step: two coupled Cullen transformations

The linear terms in $\boldsymbol{a}_o^+$, $\boldsymbol{a}_o$; $\boldsymbol{b}_0^+$, $\boldsymbol{b}_0$ in (2.3) can be eliminated by using two Cullen diagonalization transformations [32, 33, 42], separately, in their forms

$$\begin{aligned} \boldsymbol{a}_k &= \boldsymbol{f}_k + \boldsymbol{c}_k\delta_{k,0} \\ \boldsymbol{a}_k^+ &= \boldsymbol{f}_k^+ + \boldsymbol{c}_k^+\delta_{k,0} \end{aligned} \tag{3.1}$$

and

$$\begin{aligned} \boldsymbol{b}_k &= \boldsymbol{g}_k + \boldsymbol{d}_k\delta_{k,0} \\ \boldsymbol{b}_k^+ &= \boldsymbol{g}_k^+ + \boldsymbol{d}_k^+\delta_{k,0} \end{aligned} \tag{3.2}$$

where the Fourier transforms $\boldsymbol{c}_0$ and $\boldsymbol{d}_0$ represent frozen-in uniform spin deviations. In the present case, the two Cullen transformations are coupled since the non-diagonal terms $\boldsymbol{a}_k^+\boldsymbol{b}_k^+$, $\boldsymbol{a}_k\boldsymbol{b}_k$, $\boldsymbol{a}_k^+\boldsymbol{b}_k$ and $\boldsymbol{a}_k\boldsymbol{b}_k^+$ exist in Hamiltonian (2.3). The new diagonalized Hamiltonian contains $k \neq 0$ terms identical to (2.3), but with $\boldsymbol{a}_k^+$, $\boldsymbol{a}_k$; $\boldsymbol{b}_k^+$, $\boldsymbol{b}_k$ substituted by the $\boldsymbol{f}_k^+$, $\boldsymbol{f}_k$; $\boldsymbol{g}_k^+$, $\boldsymbol{g}_k$ operators and a new $k = 0$ term of the form

$$\begin{aligned} \boldsymbol{H}_0^1 &= A|c_0|^2 + A'(c_0^2 + (c_0^+)^2) + A''(c_0 + c_0^+) + B|d_0|^2 + B'(d_0^2 + (d_0^+)^2) + B''(d_0 + d_0^+) \\ &\quad + C(c_0^+d_0^+ + c_0d_0) + D(c_0^+d_0 + c_0d_0^+) \\ &= (A + 2A')c_0^2 + 2A''c_0 + (B + 2B')d_0^2 + 2B''d_0 + 2(C + D)c_0d_0. \end{aligned} \tag{3.3}$$

3.2. The second step: an extended Bogoliubov transformation

To eliminate the non-diagonal terms $\boldsymbol{f}_k\boldsymbol{g}_k^+$, $\boldsymbol{f}_k\boldsymbol{g}_k$, $\boldsymbol{f}_k^+\boldsymbol{g}_k$ and $\boldsymbol{f}_k\boldsymbol{g}_k^+$, one needs to develop an extended Bogoliubov transformation. The transformation matrix is written as

$$\begin{pmatrix} \boldsymbol{\alpha}_k^+ \\ \boldsymbol{\alpha}_k \\ \boldsymbol{\beta}_k^+ \\ \boldsymbol{\beta}_k \end{pmatrix} = \begin{pmatrix} a_{1k} & a_{2k} & a_{3k} & a_{4k} \\ a_{2k} & a_{1k} & a_{4k} & a_{3k} \\ a_{3k} & a_{4k} & a_{1k} & a_{2k} \\ a_{4k} & a_{3k} & a_{2k} & a_{1k} \end{pmatrix} \begin{pmatrix} \boldsymbol{f}_k^+ \\ \boldsymbol{f}_k \\ \boldsymbol{g}_k^+ \\ \boldsymbol{g}_k \end{pmatrix} \tag{3.4}$$

and consequently its reversed matrix $A_{jk}(j = 1, 2, 3, 4)$ [46]. This transformation is asymmetrical for the positive and negative k spaces. The transformation matrix in the $-\boldsymbol{k}$ space is:

$$\begin{pmatrix} \boldsymbol{\alpha}_{-k}^{+} \\ \boldsymbol{\alpha}_{-k} \\ \boldsymbol{\beta}_{-k}^{+} \\ \boldsymbol{\beta}_{-k} \end{pmatrix} = \begin{pmatrix} a_{1k} & -a_{2k} & a_{3k} & -a_{4k} \\ -a_{2k} & a_{1k} & -a_{4k} & a_{3k} \\ a_{3k} & -a_{4k} & a_{1k} & -a_{2k} \\ -a_{4k} & a_{3k} & -a_{2k} & a_{1k} \end{pmatrix} \begin{pmatrix} \boldsymbol{f}_{-k}^{+} \\ \boldsymbol{f}_{-k} \\ \boldsymbol{g}_{-k}^{+} \\ \boldsymbol{g}_{-k} \end{pmatrix}. \tag{3.5}$$

The problem becomes to solve the equation group (denoted as E and shown in appendix B), consisting of eight equations (i.e., (B.1)–(B.4) and (27)–(30) in [46]) and eight unknowns (i.e., a_{ik} and $A_{jk}(i = 1, 2, 3, 4;\ j = 1, 2, 3, 4)$). This is similar to that developed in a recent paper for diagonalizing the spin-wave Hamiltonian of the four sublattice systems [46]. The procedure for solving this equation group is represented in appendix C.

After performing the extended Bogoliubov transformation, the Hamiltonian (2.3) becomes

$$\begin{aligned} \boldsymbol{H} = {} & \boldsymbol{H}_0^0 + \boldsymbol{H}_0^1 + \boldsymbol{H}_0^2 + \sum_k A_{k1}\boldsymbol{\alpha}_k^+\boldsymbol{\alpha}_k + \sum_k B_{k1}\boldsymbol{\beta}_k^+\boldsymbol{\beta}_k + \sum_k A_{k2}(\boldsymbol{\alpha}_k^+\boldsymbol{\alpha}_k^+ + \boldsymbol{\alpha}_k\boldsymbol{\alpha}_k) \\ & + \sum_k B_{k2}(\boldsymbol{\beta}_k^+\boldsymbol{\beta}_k^+ + \boldsymbol{\beta}_k\boldsymbol{\beta}_k) + \sum_k A_{k3}(\boldsymbol{\alpha}_k^+\boldsymbol{\alpha}_{-k}^+ + \boldsymbol{\alpha}_k\boldsymbol{\alpha}_{-k}) \\ & + \sum_k B_{k3}(\boldsymbol{\beta}_k^+\boldsymbol{\beta}_{-k}^+ + \boldsymbol{\beta}_k\boldsymbol{\beta}_{-k}). \end{aligned} \tag{3.6}$$

The parameters $\boldsymbol{H}_0^2$, A_{ki} and $B_{ki}(i = 1, 2, 3)$ are given in appendix D. The splitting of two energy levels exists, which is ascribed to the positive and negative signs in the formula of K (see (C.6)).

3.3. The third step: two independent Bogoliubov transformations

Next, one of two Bogoliubov transformations is

$$\begin{aligned} \boldsymbol{\alpha}_k^+ &= l_{1k}\boldsymbol{\mu}_k^+ + l_{2k}\boldsymbol{\mu}_k \\ \boldsymbol{\alpha}_{-k} &= l_{1k}\boldsymbol{\mu}_{-k} - l_{2k}\boldsymbol{\mu}_{-k}^+ \end{aligned} \tag{3.7}$$

with

$$\begin{aligned} l_{1k} &= \left(\frac{1+\epsilon_k}{2\epsilon_k}\right)^{\frac{1}{2}} \\ l_{2k} &= \left(\frac{1-\epsilon_k}{2\epsilon_k}\right)^{\frac{1}{2}} \\ \epsilon_k &= \left(1 - \left(\frac{2A_{k2}}{A_{k1}}\right)^2\right)^{\frac{1}{2}} \end{aligned} \tag{3.8}$$

and the other is similar to that above.

After performing these transformations, one reduces the Hamiltonian (3.6) to

$$\begin{aligned} \boldsymbol{H} = {} & \boldsymbol{H}_0^0 + \boldsymbol{H}_0^1 + \boldsymbol{H}_0^2 + \boldsymbol{H}_0^3 + \sum_k C_{k1}\boldsymbol{\mu}_k^+\boldsymbol{\mu}_k + \sum_k D_{k1}\boldsymbol{\nu}_k^+\boldsymbol{\nu}_k + \sum_k A_{k3}(\boldsymbol{\mu}_k^+\boldsymbol{\mu}_{-k}^+ + \boldsymbol{\mu}_k\boldsymbol{\mu}_{-k}) \\ & + \sum_k B_{k3}(\boldsymbol{\nu}_k^+\boldsymbol{\nu}_{-k}^+ + \boldsymbol{\nu}_k\boldsymbol{\nu}_{-k}). \end{aligned} \tag{3.9}$$

The parameters in Hamiltonian (3.9) are not shown here for simplicity. At this step, the non-diagonal terms $\boldsymbol{\alpha}_k^+\boldsymbol{\alpha}_k^+$, $\boldsymbol{\alpha}_k\boldsymbol{\alpha}_k$, $\boldsymbol{\beta}_k^+\boldsymbol{\beta}_k^+$ and $\boldsymbol{\beta}_k\boldsymbol{\beta}_k$ are removed.

3.4. The fourth step: two independent Holstein–Primakoff transformations

Then, one needs to use two independent Holstein–Primakoff transformations to eliminate the remains of the non-diagonal terms, one of which is described as follows:

$$\begin{aligned} \boldsymbol{\mu}_k^+ &= \frac{1}{\sqrt{2}}[n_{1k}(\boldsymbol{\zeta}_k^+ + \boldsymbol{\zeta}_{-k}^+) + n_{2k}(\boldsymbol{\zeta}_k - \boldsymbol{\zeta}_{-k})] \\ \boldsymbol{\mu}_{-k} &= \frac{1}{\sqrt{2}}[n_{1k}(\boldsymbol{\zeta}_k - \boldsymbol{\zeta}_{-k}) + n_{2k}(\boldsymbol{\zeta}_k^+ + \boldsymbol{\zeta}_{-k}^+)] \end{aligned} \tag{3.10}$$

with

$$\begin{aligned} n_{1k} &= \left(\frac{1+\rho_k}{2\rho_k}\right)^{\frac{1}{2}} \\ n_{2k} &= \left(\frac{1-\rho_k}{2\rho_k}\right)^{\frac{1}{2}} \\ \rho_k &= \sqrt{1-\left(\frac{A_{k3}}{C_{k1}}\right)^2}. \end{aligned} \tag{3.11}$$

Finally, one finds

$$\boldsymbol{H} = \boldsymbol{H}_0^0 + H_0^1 + \boldsymbol{H}_0^2 + \boldsymbol{H}_0^3 + \boldsymbol{H}_0^4 + \sum_k \hbar\omega_k^{(+)}\boldsymbol{\zeta}_k^+\boldsymbol{\zeta}_k + \sum_k \hbar\omega_k^{(-)}\boldsymbol{\eta}_k^+\boldsymbol{\eta}_k. \tag{3.12}$$

Here $\boldsymbol{H}_0^0$ and $\boldsymbol{H}_0^1$ are given in (A.1) and (3.3), and other parameters are not shown for simplicity.

4. Ground state

Following the analysis in the last section, one obtains the spin-wave spectra for the present system. In this section, we will discuss briefly the ground state for different configurations.

The energy of the ground state of the present system is

$$E_0 = \boldsymbol{H}_0^0 + \boldsymbol{H}_0^1 + \boldsymbol{H}_0^2 + \boldsymbol{H}_0^3 + \boldsymbol{H}_0^4. \tag{4.1}$$

The easy direction of the magnetization can be determined by the equilibrium conditions:

$$\frac{\partial E_0}{\partial \theta_A} = 0 \tag{4.2}$$

$$\frac{\partial E_0}{\partial \theta_B} = 0 \tag{4.3}$$

and the criterion

$$\Delta = \frac{\partial^2 E_0}{\partial \theta_A^2}\frac{\partial^2 E_0}{\partial \theta_B^2} - \left(\frac{\partial^2 E_0}{\partial \theta_A\,\partial \theta_B}\right)^2 > 0. \tag{4.4}$$

4.1. In the pure classical limit

In the pure classical limit, the free energy becomes

$$\begin{aligned} E_0 = &-NZJ[S_A(S_B+1) + S_B(S_A+1)]\cos(\theta_A - \theta_B) - NK_AS_A(S_A+1)\cos^2\theta_A \\ &-NK_BS_B(S_B+1)\cos^2\theta_B \end{aligned} \tag{4.5}$$

and the equilibrium conditions of (4.2) and (4.3) yield

$$\sin 2\theta_A + y' \sin 2(\theta_A + \alpha) = 0 \tag{4.6}$$

$$-x' \sin \alpha + y' \sin 2(\theta_A + \alpha) = 0 \tag{4.7}$$

with $\alpha = \theta_B - \theta_A$ and

$$x' = -\frac{ZJ[S_A(S_B + 1) + S_B(S_A + 1)]}{K_A S_A(S_A + 1)} \tag{4.8}$$

$$y' = \frac{K_B S_B(S_B + 1)}{K_A S_A(S_A + 1)}. \tag{4.9}$$

(4.6) and (4.7) are just the same as (3.2) and (3.3) in our previous paper [5] in which the spin configurations in the absence of an external magnetic field were systematically investigated for a two-sublattice system.

Although the definitions of (4.8) and (4.9) for x' and y' differ from x and y in (3.1) of [5], the results obtained in that paper can be directly taken for the present investigation. Following the analysis in [5], one can obtain an explicit expression for the canting angle α between the two-sublattice moments:

$$\sin^2 \alpha = 1 - \frac{[x'(1 - y')]^2}{4(y'^2 - x'^2 y')}. \tag{4.10}$$

The definitions of (4.8) and (4.9) for x' and y' can be written as

$$x' = (1 + z)x \tag{4.11}$$

$$y' = zy \tag{4.12}$$

with

$$x = -\frac{ZJ}{K_A} \tag{4.13}$$

$$y = \frac{K_B}{K_A} \tag{4.14}$$

$$z = \frac{S_B(S_B + 1)}{S_A(S_A + 1)} \tag{4.15}$$

Then the conditions for non-collinear configurations obtained by the spin-wave theory are

$$-\frac{2yz}{(1 + yz)(1 + z)} \leqslant x \leqslant \frac{2yz}{(1 + yz)(1 + z)} \qquad \text{if } y < -\frac{1}{z} \tag{4.16}$$

$$\frac{2yz}{(1 + yz)(1 + z)} \leqslant x \leqslant -\frac{2yz}{(1 + yz)(1 + z)} \qquad \text{if } 0 > y > -\frac{1}{z}. \tag{4.17}$$

The phase diagrams of the spin configurations at zero field, obtained by the spin-wave theory, are represented in figure 1. Comparing with the results obtained by the mean-field theory [5], one finds that the difference between the spin amplitudes of the two-sublattices affects the border of the different spin configurations. If there is no difference between the spin amplitudes, i.e., in the case of $z = 1$, the spin-wave results will be the same as the mean-field ones.

Our results above differ from those obtained by del Moral [32], who argued that classically second-order anisotropy terms alone are unable to produce a continuous spin canting angle. The main reason is that the del Moral paper [32] was actually based on a one-sublattice model. Our results indicate that continuous transitions occur in the two-sublattice systems, accompanied with the continuous change of the angle between the averaged sublattice magnetizations.

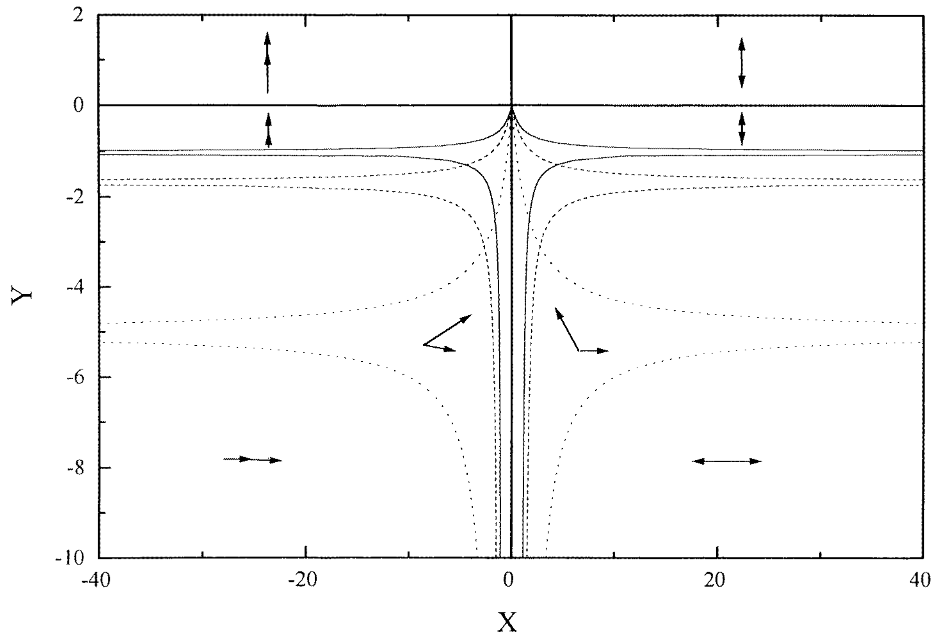

Figure 1. A phase diagram of the spin configurations in a two-sublattice system, derived by means of the spin-wave theory. x, y and z are defined in (4.13)–(4.15). The border between the different spin configurations is described by (4.16) and (4.17). The solid, the dashed and the dotted lines correspond to $z = 1$, 0.6 and 0.2, respectively. The parameters in the phase diagram cover those of all R–T compounds when only the second-order anisotropies are considered.

4.2. The quantum effects

4.2.1. Easy axis. The easy axis configurations are collinear. $A'' = B'' = 0$ so that $\boldsymbol{H}_0^1 = \mathbf{0}$, and $A' = B' = 0$. This makes the second and third steps of the diagonalizing procedure in the last section unnecessary and thus $\boldsymbol{H}_0^3 = \boldsymbol{H}_0^4 = \mathbf{0}$. The energy of the ground state for ferromagnets is

$$E_0 = \boldsymbol{H}_0^0 + \boldsymbol{H}_0^2 = -NZJS_A(S_B+1) - NZJS_B(S_A+1) - NK_AS_A(S_A+1) \\ -NK_BS_B(S_B+1) \qquad (4.18a)$$

including the energy of the original state, only. The energy of the ground state for ferrimagnets is

$$E_0 = \boldsymbol{H}_0^0 + \boldsymbol{H}_0^2 = -NZ|J|S_A(S_B+1) - NZ|J|S_B(S_A+1) - NK_AS_A(S_A+1) \\ -NK_BS_B(S_B+1) \\ +\sum_k \sqrt{(Z|J|(S_A+S_B) + K_AS_A + K_BS_B)^2 - 4Z^2J^2S_AS_B\gamma_k^2} \qquad (4.18b)$$

which includes the energies of the original state and zero-point quantum fluctuations.

4.2.2. Easy plane and easy cone. The easy cone configuration is very complicated: the average magnetization directions of the two-sublattice are not collinear. In this case, all parameters A', B', A'' and B'' are not equal to zero and all terms in Hamiltonians (3.4) remain. The energies of the ground states are functions of the angles θ_A and θ_B. There is no simple form for the energy of the ground state of the easy cone configuration and one needs to list all terms of E_0 in (4.1).

To simplify, in this paper, we only show the results obtained in the large-exchange limit, which are appropriate for the districts close to the borders between the collinear and non-collinear spin structures. These results are suitable for the easy plane configurations, by extrapolating $\theta_A = \theta_B = \pi/2$ (or $\theta_A = \theta_B = 3\pi/2$) for ferromagnets and $\theta_A = \pi/2$ and $\theta_B = 3\pi/2$ (or $\theta_A = 3\pi/2$ and $\theta_B = \pi/2$) for ferrimagnets. One has

$$E_0 = \boldsymbol{H}_0^0 + \boldsymbol{H}_0^1 + \boldsymbol{H}_0^2 + \boldsymbol{H}_0^3 + \boldsymbol{H}_0^4 = E_0' + \frac{1}{2}\sum_k \sqrt{(\Omega_k - \Gamma_k + \Delta_1)(\Omega_k + \Gamma_k + \Delta_2)} + \frac{1}{2}\sum_k \sqrt{(\Omega_k - \Gamma_k - \Delta_1)(\Omega_k + \Gamma_k - \Delta_2)}. \tag{4.19}$$

The parameters in (4.19) are shown in appendix E. Equation (4.19) consists of the energies of the original state and the zero-point quantum fluctuations and the uniform ($\boldsymbol{k} = \boldsymbol{0}$) spin canting fluctuations from the c axis. Similar to the del Moral results [32], the uniform ($\boldsymbol{k} = \boldsymbol{0}$) spin canting fluctuations represent a spin reorientation from the c axis at 0 K due to the quantum fluctuations.

The equilibrium directions of the magnetization are determined by the equilibrium conditions, shown in (4.2) and (4.3), which usually cannot be solved analytically so a numerical method must be used. The criterion of (4.4) is necessary for determining the minimum state of the system. One should keep in mind that the equations (4.19) and (E.1)–(E.5) were derived in the large-exchange limit, and are only suitable for the easy plane or for the easy cone zones near to the border lines between the collinear and non-collinear spin configurations. Nevertheless, these results can be used to determine the border lines approximately (here we omitted them to avoid numerousness in algebra). This confirms that the continuous transitions still exist.

5. Spin-wave excitation

In this section, the spin-wave excitation will be discussed for different ground states.

5.1. Easy axis

When the ground state is of the easy axis configuration, the spin-wave spectra of the present system are

$$\hbar\omega_k^{(\pm)} = \pm\sqrt{(Z|J|(S_B - S_A) + K_A S_A - K_B S_B)^2 + 4Z^2J^2 S_A S_B \gamma_k^2} + [Z|J|(S_A + S_B) + K_A S_A + K_B S_B] \tag{5.1a}$$

and

$$\hbar\omega_k^{(\pm)} = \sqrt{(Z|J|(S_A + S_B) + K_A S_A + K_B S_B)^2 - 4Z^2J^2 S_A S_B \gamma_k^2} \pm [Z|J|(S_B - S_A) + K_A S_A - K_B S_B] \tag{5.1b}$$

for ferromagnetic and ferrimagnetic materials respectively. Some examples for the spin-wave dispersions are shown in figures 2(a) and (b), respectively, for ferromagnets and ferrimagnets. For comparison, we list here experimental data for some R–T compounds: $Ho_2Co_{14}Fe_3$, $n_{RT} = 0.54$ kg T A^{-1} m^{-2}, $M_R = 84.5$ A m^2 kg^{-1}, $M_T = 130.2$ A m^2 kg^{-1}, $K_1^T = 220$ J kg^{-1}, $K_1^R = -760$ J kg^{-1}, $K_2^R = 60$ J kg^{-1} [47]; $Nd_2Fe_{14}B$, $n_{RT} = 1.0$ kg T A^{-1} m^{-2}, $M_R = 16.4$ A m^2 kg^{-1}, $M_T = 175.9$ A m^2 kg^{-1}, $K_1^T = 119$ J kg^{-1},

$K_1^R = -3270$ J kg^{-1}, $K_2^R = 7840$ J kg^{-1}, $K_3^R = -3500$ J kg^{-1} [48]. The spin-wave spectra are very sensitive to the strength of the anisotropies, the exchange constant and the spin amplitudes. For certain values of the parameters, the frequencies of two branches of the spin waves decrease (or increase) with increasing value of γ_k^2 in the same trend. The splittings of the spin-wave spectra always exist for ferromagnets, and, with the exception of

$$Z|J|(S_B - S_A) + K_A S_A - K_B S_B = 0 \tag{5.2}$$

for ferrimagnets. The conditions for the presence of the acoustic branch of the spin-waves are

$$(ZJS_B + K_A S_A)(ZJS_A + K_B S_B) \pm Z^2 J^2 S_A S_B = 0. \tag{5.3}$$

The upper sign is for the ferromagnet while the lower sign is for the ferrimagnet. In other cases, the $k = 0$ gap always exists and thus the two branches of the spin-wave spectra are optical. It is understood that the single-ion uniaxial and/or non-uniaxial anisotropy is favourable to the relative motion of the spins for ferromagnetic and ferrimagnetic two-sublattice structures.

For some values of the anisotropies, as shown in figure 2(b), the frequencies of the spin waves in ferrimagnets become soft in the vicinity of the centre of the Brillouin zone. Furthermore, imaginary frequencies can appear in the vicinity of the centre of the Brillouin zone. The quantum fluctuations shift the sublattice configuration from the classical configuration, even at 0 K if the following condition is satisfied:

$$Z|J|(S_A + S_B) + K_A S_A + K_B S_B + 2Z|J|\sqrt{S_A S_B}\gamma_k \geqslant 0. \tag{5.4}$$

$$Z|J|(S_A + S_B) + K_A S_A + K_B S_B - 2Z|J|\sqrt{S_A S_B}\gamma_k \leqslant 0. \tag{5.5}$$

This vicinity may be extended to nearly fill out the Brillouin zone (except for $\gamma_k = 0$) so that the real frequency of the spin-waves only appears on the boundary of the Brillouin zone in the following condition:

$$Z|J|(S_A + S_B) + K_A S_A + K_B S_B = 0. \tag{5.6}$$

5.2. *Easy plane and easy cone*

The spin-wave spectra of the easy plane ground state or the easy cone one (in the large-exchange limit) may be written as

$$\hbar\omega_k^{(\pm)} = \sqrt{(\Omega_k - \Gamma_k \pm \Delta_1)(\Omega_k + \Gamma_k \pm \Delta_2)}. \tag{5.7}$$

The parameters in (5.7) are the same as those defined in (E.2)–(E.5).

When $\Delta_1 = \Delta_2 = 0$, i.e., the conditions of

$$Z|J|(S_A \pm S_B)\cos(\theta_A - \theta_B) + K_A S_A \cos^2\theta_A + K_B S_B \cos 2\theta_B = 0 \tag{5.8}$$

and

$$K_A S_A \sin^2\theta_A - K_B S_B \sin^2\theta_B = 0 \tag{5.9}$$

are satisfied, the splitting of the spin-wave spectra is removed. The conditions for the presence of the acoustic branch of the spin-waves are

$$\Omega_0 - \Gamma_0 \pm \Delta_1 = 0 \tag{5.10}$$

or

$$\Omega_0 + \Gamma_0 \pm \Delta_2 = 0 \tag{5.11}$$

where Ω_0 and Γ_0 are values of Ω_k and Γ_k in (E.2) and (E.3), for $k = 0$.

The conditions for the imaginary frequencies are

$$(\Omega_k - \Gamma_k \pm \Delta_1)(\Omega_k + \Gamma_k \pm \Delta_2) \leqslant 0. \tag{5.12}$$

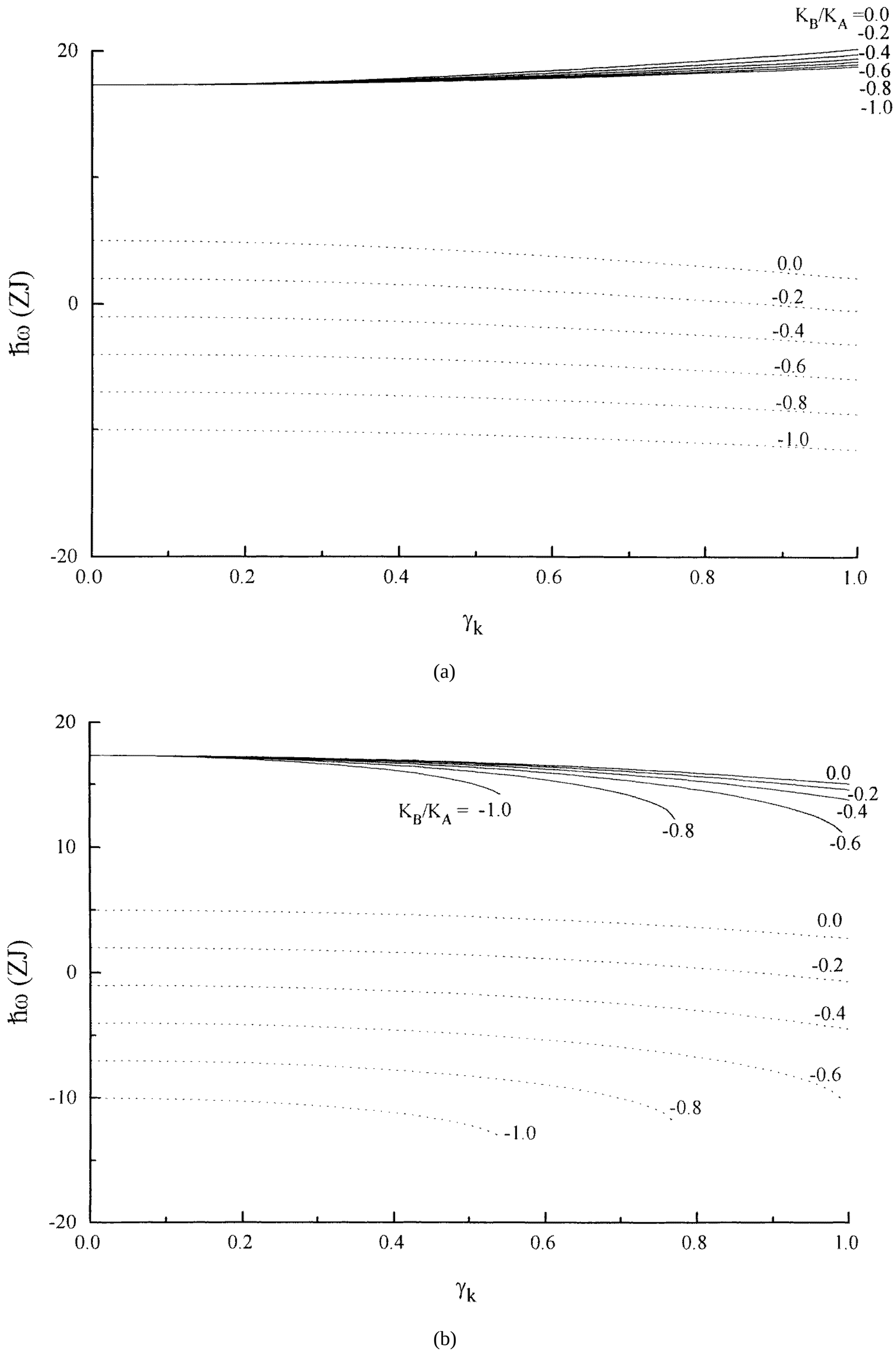

Figure 2. Spin-wave dispersions of the easy axis configurations in a two-sublattice system, described by (5.1*a*) and (5.1*b*) respectively for (a) ferromagnetic and (b) ferrimagnetic materials. The solid and the dotted lines correspond to the spin-wave spectra $\hbar\omega_k^+$ and $\hbar\omega_k^-$, respectively. The parameters used are $S_A = 5/2$, $S_B = 9/2$. $Z = 6$, $J = 1$, $K_A = 10$.

6. Sublattice magnetization and specific heat at low temperatures

The sublattice magnetization and specific heat at low temperature are interesting subjects of many investigations. In this section, we shall discuss briefly these topics for different ground states.

6.1. Easy axis

For easy axis ferromagnets, it can be seen, from (4.18a), there is no quantum fluctuation as well as the deviation to the original state at 0 K.

For easy axis ferrimagnets, in practice, the fourth term in E_0 of (4.18b) represents the deviation to the original state at 0 K. Following the normal procedure, one obtains the deviation of the sublattice magnetization at 0 K of the present ferrimagnetic Heisenberg system:

$$\Delta\Gamma_A^z = \Delta\Gamma_B^z = \frac{1}{2}\sum_k\left[\frac{1}{\sqrt{1-\gamma_k'^2}} - 1\right]$$
$$= \frac{1}{2}\sum_k\left[\left(\sqrt{1-\frac{4Z^2J^2S_AS_B\gamma_k^2}{(Z|J|(S_A+S_B)+K_AS_A+K_BS_B)^2}}\right)^{-1} - 1\right]. \tag{6.1}$$

The deviation of the sublattice magnetization is decreased by means of the anisotropies in comparison with that of the usual Heisenberg antiferromagnetic system. When the frequencies of the spin-wave modes are imaginary, the deviation of the sublattice magnetization is also smaller than that of the usual system. In the limiting cases of (5.6), the spin-wave excitation only exists near the boundary of the Brillouin zone and then the deviation of the sublattice magnetization at 0 K becomes quite small.

The temperature dependence of the magnetization may be re-evaluated by

$$\Delta M(T) = M(0) - M(T) = \frac{M(0)}{N|S_A \pm S_B|}\sum_k \langle n_k\rangle_T$$
$$= \frac{M(0)}{N|S_A \pm S_B|}\left[\sum_k\langle\xi_k^+\xi_k\rangle_T + \sum_k\langle\eta_k^+\eta_k\rangle_T\right]. \tag{6.2}$$

Here positive and negative signs correspond to ferromagnets and ferrimagnets, respectively. For low temperatures ($X = \hbar\omega/k_BT \gg 1$), replacing the Bose factor $1/(e^x - 1)$ by e^{-x} is valid in the long-wavelength region of momentum integration. Focusing on the districts in the vicinity of the centre of the Brillouin zone, one finds that the temperature dependence of the magnetization at low temperatures of the present system is the same as the Bloch $T^{3/2}$ law in a ferromagnet. For the ferromagnets, the term contributed by the lower energy level $\hbar\omega_k^-$ is dominant, but for the ferrimagnets, the temperature dependence of the magnetization can be dominated by the term of $\hbar\omega_k^-$ and $\hbar\omega_k^+$, depending on which level is lower. Similarly, the internal energy and the specific heat at low temperatures of the present system satisfy the $T^{5/2}$ and the $T^{3/2}$ laws, respectively. These temperature behaviours are similar to those of a ferromagnet, due to the effect of the different sublattice anisotropies and/or the different spin amplitudes.

In the region where the frequencies of the spin-waves are imaginary, the calculation for the temperature behaviours of the physical quantities cannot be performed under the assumption of the long-wavelength approximation and becomes much more difficult.

6.2. Easy plane and easy cone

For the easy plane (or easy cone) spin structure, the deviation of the sublattice magnetizations is controlled by the zero-point quantum fluctuation and the uniform ($k = 0$) spin canting fluctuation shown in section 4.2.2. The temperature dependence of the magnetization, the internal energy and the specific heat at low temperatures can be derived from the spin-wave spectra obtained in section 5.2. The free energy of the system can be described by

$$E = E_0 + E_k(T) = E_0 - k_B T \ \ln \prod_k \frac{1}{1 - \exp(-\varepsilon_k / k_B T)} \tag{6.3}$$

where E_0 includes the contributions of the static ground-state energy (consisting of the original-state energy and the uniform ($k = 0$) spin canting fluctuation energy) and the zero-point quantum fluctuation energy. $E_k(T)$ is the free energy of a thermally excited magnon.

The free energy E of the system is a function of the order parameters θ_A and θ_B (or α). The minimization of the free energy E gives the solutions for the equilibrium values of the order parameters at finite temperatures. One may analyse the temperature dependence of the order parameters θ_A and θ_B (or α) at low temperatures. Spin-reorientation transition with the change of the canting angle α between the averaged sublattice moments can be demonstrated, which is characteristic of two-sublattice systems. The physical contents of the spin-reorientation transition in the present two-sublattice system are different from those in the del Moral model [32, 33]. However, the representations of these properties are very complicated and, usually, a numerical method with the aid of a computer is needed.

7. Concluding remarks

The main results obtained in this work may be listed as follows.

(1) The degeneracy of the spin-wave spectrum of a normal Heisenberg ferromagnet or antiferromagnet can be removed by the different sublattice anisotropies and/or the different spin amplitudes.

(2) Gaps can appear in the spin-wave spectra, depending on the competition among the exchange and the anisotropies. In most cases of the present system, only the optical branches of the spin-waves can be excited and the spins favour the relative motion in presence of the anisotropies.

(3) In some cases, the spin-wave mode becomes soft and gains imaginary frequencies close to the centre of the Brillouin zone at low temperatures.

(4) The ground states of the easy axis, the easy plane and the easy cone configurations were discussed briefly. The border lines between the different spin structures in the pure classical limit were derived to be similar to those obtained based on a mean-field two-sublattice model. The difference between the spin amplitudes of the two sublattices affects the border of the spin configurations. The continuous transitions, accompanied with the continuous change of the angle between the sublattice magnetizations, were found to occur in either the pure classical limit or the large-exchange limit.

(5) There is no deviation of the sublattice magnetization in the easy axis Heisenberg ferromagnets. The deviation of the sublattice magnetization of the Heisenberg ferrimanget at 0 K is decreased by the effect of the anisotropies. Under a certain condition, such deviation becomes quite small.

(6) The temperature dependences of the magnetization and the specific heat of the easy axis configurations satisfy the Bloch $T^{3/2}$ laws. A numerical calculation is needed for the

representation of the temperature dependence of the properties of the easy plane and the easy cone configurations.

Acknowledgments

This work has been supported by the National Natural Science Foundation of China, by the President Foundation of Chinese Academy of Sciences and by the Science and Technology Commission of Liaoning and Shenyang.

Appendix A. Transformation of spin vector coordinates

After performing the transformation of spin vector coordinates as described in [32, 33, 44, 45] and using the Holstein–Primakoff transform [41] and the linear-spin-wave approximation [34, 35], one rewrites the Hamiltonian (2.1) as (2.2). The parameters defined in (2.2) are

$$\boldsymbol{H}_0^0 = -2NZS_AS_BJ\,\cos(\theta_A-\theta_B) - N\sum_{i=A,B} K_i\left(S_i^2\,\cos^2\,\theta_i + \frac{S_i}{2}\,\sin^2\,\theta_i\right) \tag{A.1}$$

$$A = 2ZJS_B\,\cos(\theta_A-\theta_B) - K_AS_A(3\,\sin^2\,\theta_A - 2) \tag{A.2}$$

$$B = 2ZJS_A\,\cos(\theta_A-\theta_B) - K_BS_B(3\,\sin^2\,\theta_B - 2) \tag{A.3}$$

$$C = -ZJ\sqrt{S_AS_B}(\cos(\theta_A-\theta_B) - 1) \tag{A.4}$$

$$D = -ZJ\sqrt{S_AS_B}(\cos(\theta_A-\theta_B) + 1) \tag{A.5}$$

$$A' = -\tfrac{1}{2}K_AS_A\,\sin^2\,\theta_A \tag{A.6}$$

$$B' = -\tfrac{1}{2}K_BS_B\,\sin^2\,\theta_B \tag{A.7}$$

$$A'' = \sqrt{2NS_A}(K_AS_A\,\sin\theta_A\,\cos\,\theta_A + JS_B\,\sin(\theta_A-\theta_B)) \tag{A.8}$$

$$B'' = \sqrt{2NS_B}(K_BS_B\,\sin\theta_B\,\cos\,\theta_B + JS_A\,\sin(\theta_A-\theta_B)). \tag{A.9}$$

Appendix B. The equation group E

The commutation relations of the new operators α_k^+, β_k^+, α_k, β_k result in two equations:

$$a_{1k}^2 + a_{3k}^2 - a_{2k}^2 - a_{4k}^2 = 1 \tag{B.1}$$

and

$$a_{1k}a_{3k} - a_{2k}a_{4k} = 0. \tag{B.2}$$

To eliminate the non-diagonal terms of $\alpha_k^+\beta_k^+$, $\alpha_k\beta_k$, $\alpha_k^+\beta_k$ and $\alpha_k\beta_k^+$, one needs to establish the following two equations:

$$(A+B)(A_{1k}A_{4k}+A_{2k}A_{3k})+\gamma_k[C(A_{1k}^2+A_{2k}^2+A_{3k}^2+A_{4k}^2)+2D(A_{1k}A_{2k}+A_{3k}A_{4k})] = 0 \tag{B.3}$$

$$(A+B)(A_{1k}A_{3k}+A_{2k}A_{4k})+\gamma_k[2C(A_{1k}A_{2k}+A_{3k}A_{4k})+D(A_{1k}^2+A_{2k}^2+A_{3k}^2+A_{4k}^2)] = 0 \tag{B.4}$$

and the relations between the parameters a_{ik} and A_{jk} are the same as those of (27)–(30) in [46].

Appendix C. Procedure for solving the equation group E

The equation group E, consisting of (B.1)–(B.4) and (27)–(30) of [46], can be solved by the following procedure. Using the relation of (B.1), one may rewrite (27)–(30) of [46]. For instance, (27) of [46] becomes

$$A_{1k} = \frac{1}{Y}[a_{1k} + 2a_{3k}(a_{2k}a_{4k} - a_{1k}a_{3k})]. \tag{C.1}$$

Then considering (B.2), one immediately obtains

$$A_{ik} = \frac{a_{ik}}{Y} \qquad (i = 1, 3) \tag{C.2}$$

$$A_{ik} = -\frac{a_{ik}}{Y} \qquad (i = 2, 4). \tag{C.3}$$

(B.3) minus (B.4) results in

$$(C - D)\gamma_k(a_{1k} + a_{2k})^2 - (A + B)(a_{1k} + a_{2k})(a_{3k} + a_{4k}) + (C - D)\gamma_k(a_{3k} + a_{4k})^2 = 0. \tag{C.4}$$

When $C \neq D$, (C.4) is equal to

$$a_{1k} + a_{2k} = K(a_{3k} + a_{4k}). \tag{C.5}$$

Here

$$K = \frac{1 \pm \sqrt{1 - X^2}}{X} \tag{C.6}$$

with

$$X = \frac{2(C - D)\gamma_k}{A + B}. \tag{C.7}$$

Now the equation group becomes (B.1), (B.2), (C.2), (C.3), (C.5) and one of (B.3) and (B.4).

From (B.1) and (C.5), one has

$$a_{1k} = \frac{K^2 - 1}{2K}a_{3k} + \frac{K^2 + 1}{2K}a_{4k} + \frac{1}{2K(a_{3k} + a_{4k})}. \tag{C.8}$$

Putting (C.5) into (B.2), one obtains:

$$a_{1k} = Ka_{4k} \qquad \text{if } a_{3k} + a_{4k} \neq 0. \tag{C.9}$$

Combining (C.8) and (C.9) leads to

$$a_{1k} = \pm K\sqrt{\frac{1}{K^2 - 1} + a_{3k}^2}. \tag{C.10}$$

Combining (C.9) with (B.2) results in

$$a_{2k} = Ka_{3k}. \tag{C.11}$$

Inserting (C.9)–(C.11) into (B.3), one finally finds

$$a_{1k} = \pm K\sqrt{\frac{-\sqrt{N^2 - M^2} \pm N}{2(1 - K^2)\sqrt{N^2 - M^2}}} \tag{C.12}$$

$$a_{2k} = \pm K\sqrt{\frac{\sqrt{N^2 - M^2} \pm N}{2(1 - K^2)\sqrt{N^2 - M^2}}} \tag{C.13}$$

$$a_{3k} = \pm\sqrt{\frac{\sqrt{N^2 - M^2} \pm N}{2(1 - K^2)\sqrt{N^2 - M^2}}} \tag{C.14}$$

$$a_{4k} = \pm\sqrt{\frac{-\sqrt{N^2 - M^2} \pm N}{2(1 - K^2)\sqrt{N^2 - M^2}}} \tag{C.15}$$

or other four groups of solutions $a'_{1k} = -a_{1k}$, $a'_{2k} = a_{2k}$, $a'_{3k} = a'_{3k}$, $a_{4k} = -a_{2k}$ with

$$M = C\gamma_k(K^2 + 1) - (A + B)K \tag{C.16}$$

$$N = D\gamma_k(K^2 + 1). \tag{C.17}$$

It is evident that the solutions of (C.12)–(C.15) satisfy the equation group E and that one has $Y = 1$, and thus $A_{1k} = a_{1k}$, $A_{2k} = -a_{2k}$, $A_{3k} = a_{3k}$ and $A_{4k} = -a_{4k}$. There are eight groups of solutions in (C.12)–(C.15), in accordance with different signs in the equations, which are equal for diagonalizing Hamiltonian (2.3).

Appendix D. Parameters in Hamiltonians in (3.6)

The parameters $\boldsymbol{H}_0^2$, A_{ki} and $B_{ki}(i = 1, 2, 3)$ in Hamiltonian (3.6) are as follows:

$$\boldsymbol{H}_0^2 = (A + B)(a_{2k}^2 + a_{4k}^2) - 2C\gamma_k(a_{1k}a_{4k} + a_{2k}a_{3k}) + 2D\gamma_k(a_{1k}a_{3k} + a_{2k}a_{4k}) \tag{D.1}$$

$$A_{k1} = A(a_{1k}^2 + a_{2k}^2) + B(a_{3k}^2 + a_{4k}^2) - 2C\gamma_k(a_{1k}a_{4k} + a_{2k}a_{3k}) + 2D\gamma_k(a_{1k}a_{3k} + a_{2k}a_{4k}) \tag{D.2}$$

$$B_{k1} = A(a_{3k}^2 + a_{4k}^2) + B(a_{1k}^2 + a_{2k}^2) - 2C\gamma_k(a_{1k}a_{4k} + a_{2k}a_{3k}) + 2D\gamma_k(a_{1k}a_{3k} + a_{2k}a_{4k}) \tag{D.3}$$

$$A_{k2} = -Aa_{1k}a_{2k} - Ba_{3k}a_{4k} + C\gamma_k(a_{1k}a_{3k} + a_{2k}a_{4k}) - D\gamma_k(a_{1k}a_{4k} + a_{2k}a_{3k}) \tag{D.4}$$

$$B_{k2} = -Aa_{3k}a_{4k} - Ba_{1k}a_{2k} + C\gamma_k(a_{1k}a_{3k} + a_{2k}a_{4k}) - D\gamma_k(a_{1k}a_{4k} + a_{2k}a_{3k}) \tag{D.5}$$

$$A_{k3} = A'(a_{1k}^2 - a_{2k}^2) + B'(a_{3k}^2 - a_{4k}^2) \tag{D.6}$$

$$B_{k3} = A'(a_{3k}^2 - a_{4k}^2) + B'(a_{1k}^2 - a_{2k}^2). \tag{D.7}$$

Appendix E. Parameters in Hamiltonians in section 4

The parameters in (4.19) are

$$\begin{aligned} E'_0 = &-NZJ[S_A(S_B + 1) + S_B(S_A + 1)]\cos(\theta_A - \theta_B) - N\sum_{i=A,B} K_i S_i(S_i + 1)\cos^2\theta_i \\ &+(2ZJS_B\cos(\theta_A - \theta_B) - K_A S_A(3\sin^2\theta_A - 2))|c_0|^2 \\ &+(2ZJS_A\cos(\theta_A - \theta_B) - K_B S_B(3\cos^2\theta_B - 2))|d_0|^2 \\ &-\frac{1}{2}K_A S_A\sin^2\theta_A(c_0^2 + (c_0^+)^2) - \frac{1}{2}K_B S_B\sin^2\theta_B(d_0^2 + (d_0^+)^2) \\ &+\sqrt{2NS_A}(K_A S_A\sin\theta_A\cos\theta_A + S_B J\sin(\theta_A - \theta_B))(c_0 + c_0^+) \\ &+\sqrt{2NS_B}(K_B S_B\sin\theta_B\cos\theta_B + S_A J\sin(\theta_A - \theta_B))(d_0 + d_0^+) \end{aligned} \tag{E.1}$$

$$\begin{aligned} \Omega_k = \Bigg[\Bigg(&ZJ(S_B \pm S_A)\cos(\theta_A - \theta_B) \\ &-\frac{1}{2}\sum_{i=A,B} K_i S_i(3\sin^2\theta_i - 2)\Bigg)^2 \pm (\cos(\theta_A - \theta_B) \pm 1)^2 Z^2 J^2 S_A S_B \gamma_k^2\Bigg]^{\frac{1}{2}} \end{aligned} \tag{E.2}$$

$$\Gamma_k = \frac{1}{4\Omega_k}\bigg[ZJ(S_B \pm S_A)\cos(\theta_A - \theta_B) - \frac{1}{\sum_{i=A,B} K_i S_i (3\sin^2\theta_i - 2)}\bigg](K_A S_A \sin^2\theta_A \pm K_B S_B \sin^2\theta_B) \tag{E.3}$$

$$\Delta_1 = ZJ(S_B \pm S_A)\cos(\theta_A - \theta_B) - \frac{1}{4}(7K_A S_A \sin^2\theta_A + 5K_B S_B \sin^2\theta_B) + K_A S_A + K_B S_B \tag{E.4}$$

$$\Delta_2 = ZJ(S_B \pm S_A)\cos(\theta_A - \theta_B) - \frac{1}{4}(5K_A S_A \sin^2\theta_A + 7K_B S_B \sin^2\theta_B) + K_A S_A + K_B S_B \tag{E.5}$$

where the upper signs correspond to the ferromagnets and the lower signs are for the ferrimagnets.

References

[1] Buschow K H J 1983 *Handbooks on Ferromagnetic Materials* ed E P Wohlfarth (Amsterdam: North-Holland) vol 1, 297, vol 4, p 1
[2] Rinaldi S and Pareti L 1979 *J. Appl. Phys.* **50** 7719
[3] Sarkis A and Callen E 1982 *Phys. Rev.* B **26** 3870
[4] Zhang Zhi-dong, Zhao Tong, Sun X K and Chuang Y C 1992 *J. Appl. Phys.* **71** 3434
[5] Zhang Zhi-dong, Zhao Tong, de Châtel P F and de Boer F R 1995 *J. Magn. Magn. Mater.* **147** 74
[6] Zhang Zhi-dong, Zhao Tong, de Châtel P F and de Boer F R *J. Magn. Magn. Mater.* at press
[7] Herbst J F 1991 *Rev. Mod. Phys.* **63** 819
[8] Li S H and Coey J M D 1991 *Handbooks on Magnetic Materials* ed K H J Buschow (Amsterdam: North-Holland) vol 6, p 1
[9] Ibarra M R, Algarabel P A, Marquina C, Arnaudas J I, del Moral A, Pareti L, Moze O, Maruzi G and Solzi M 1989 *Phys. Rev.* B **39** 7081
[10] Yamada M, Kato H, Yamamoto H and Nakagawa Y 1988 *Phys. Rev.* B **38** 620
[11] Selke W 1988 *Phys. Rep.* **170** 213
[12] Yamada Y and Hamaya N 1983 *J. Phys. Soc. Japan* **52** 3466
[13] Selke W, Barreto M and Yeomans J 1985 *J. Phys. C: Solid State Phys.* **18** L393
[14] Igarashi J 1992 *Phys. Rev.* B **46** 10 763
[15] Queriroz C A and Figueiredo W 1987 *Phys. Rev.* B **37** 5544
[16] Endo Y and Ayukawa T 1989 *J. Phys. Soc. Japan* **58** 2515
[17] Gopalan S and Cottam M G 1990 *Phys. Rev.* B **42** 624
[18] Niira K 1960 *Phys. Rev.* **117** 129
[19] Cooper B R, Elliott R J, Nettel S J and Suhl H 1962 *Phys. Rev.* **127** 57
[20] Kaplan T A and Lyons D H 1963 *Phys. Rev.* **129** 2072
[21] Ozhogin V I 1965 *Sov. Phys.–JETP* **21** 874
[22] Bar'yakhtar V G and Kvirikadze G A 1965 *Sov. Phys.–Solid State* **7** 891
[23] Bar'yakhtar V G and Maleev S V 1965 *Sov. Phys.–Solid State* **5** 858
[24] Lindgard P A, Kowalska A and Laut P 1967 *J. Phys. Chem. Solids* **28** 1357
[25] Cooper B R 1968 *Phys. Rev.* **169** 281
[26] Brooks M S S, Goodings D A and Ralph H I 1968 *J. Phys. C: Solid State Phys.* **1** 132
[27] Brooks M S S 1970 *Phys. Rev.* B **1** 2257
[28] Brooks M S S and Egami T 1973 *J. Phys. C: Solid State Phys.* **6** 513
[29] Brooks M S S and Egami T 1973 *J. Phys. C: Solid State Phys.* **6** 3719
[30] Lindgard P A and Danielsen O 1974 *J. Phys. C: Solid State Phys.* **7** 1523
[31] Lindgard P A and Danielsen O 1975 *Phys. Rev.* B **11** 351
[32] del Moral A 1992 *J. Phys.: Condens. Matter* **4** 4687
[33] del Moral A 1992 *J. Phys.: Condens. Matter* **4** 4703
[34] Anderson P W 1952 *Phys. Rev.* **86** 694
[35] Kubo R 1952 *Phys. Rev.* **87** 568
[36] Oitmaa J and Betts D D 1978 *Can. J. Phys.* **56** 897

[37] Tang S and Hirsh J E 1989 *Phys. Rev.* B **39** 4548
[38] Gross M, Sanchez-Velasco E and Siggia E D 1989 *Phys. Rev.* B **40** 11 328
[39] Huse D A and Elser V 1988 *Phys. Rev. Lett.* **60** 2531
[40] Jacobs I S 1961 *J. Appl. Phys.* **32** 61S
[41] Holstein T and Primakoff H 1940 *Phys. Rev.* **58** 1098
[42] Cullen J 1987 *J. Appl. Phys.* **61** 4413
[43] Bogoliubov N N 1947 *J. Phys. USSR* **11** 23
[44] Rudowicz C 1985 *J. Phys. C: Solid State Phys.* **18** 1415
[45] Buckmaster H A 1962 *Can. J. Phys.* **40** 1670
[46] Zhang Zhi-dong 1996 *Phys. Rev.* B **53** 2569
[47] Sinnema S 1988 *PhD Thesis* University of Amsterdam
[48] Verhoef R 1990 *PhD Thesis* University of Amsterdam